Orientation Controlled Anisotropy in Single Crystals of Quasi-1D $BaTiS_3$

Boyang Zhao[1†], Md Shafkat Bin Hoque[2†], Gwan Yeong Jung[3], Hongyan Mei[4], Shantanu Singh[1], Guodong Ren[5], Milena Milich[2], Qinai Zhao[1], Nan Wang[1], Huandong Chen[1], Shanyuan Niu[1‡], Sang-Jun Lee[6], Cheng-Tai Kuo[6], Jun-Sik Lee[6], John A. Tomko[2], Han Wang[1,7], Mikhail A. Kats[4], Rohan Mishra[3,5], Patrick E. Hopkins[2,8,9] and Jayakanth Ravichandran[1,7*]

[1]*Mork Family Department of Chemical Engineering and Materials Science, University of Southern California, Los Angeles, California, 90089, USA*

[2]*Department of Mechanical and Aerospace Engineering, University of Virginia, Charlottesville, Virginia, 22904, USA*

[3]*Department of Mechanical Engineering and Material Science, Washington University in St. Louis, St. Louis, MO, 63130, USA*

[4]*Department of Electrical and Computer Engineering, University of Wisconsin–Madison, Madison, WI, 53706, USA.*

[5]*Institute of Materials Science and Engineering, Washington University in St. Louis, St. Louis, MO, 63130, USA*

[6]*Stanford Synchrotron Radiation Lightsource, SLAC National Accelerator Laboratory, Menlo Park, CA 94025, USA.*

[7]*Ming Hsieh Department of Electrical Engineering, University of Southern California, Los Angeles, California, 90089, USA*

[8]*Department of Materials Science and Engineering, University of Virginia, Charlottesville, Virginia, 22904, USA*

[9]*Department of Physics, University of Virginia, Charlottesville, Virginia, 22904, USA*

[†]*These authors contributed equally: Boyang Zhao, Md Shafkat Bin Hoque.*

[*] *j.ravichandran@usc.edu*

Present Address:

[‡]*College of Engineering and Applied Sciences, National Laboratory of Solid State Microstructures, Nanjing University, China, 210093.*

Supporting Information

I. Structure configurations of BTS crystals

Figure S1 shows a) BTS needle, b) BTS (100) and c) BTS (001). The orientation determined by XRD are also plotted next to the crystal. Optical images of BTS crystals are obtained using an Olympus BX51 microscope.

BTS needle takes the form of a one-dimensional needle. Its *c*-axis is parallel to the long axis (along the length of the needle), and *a*-axis and *b*-axis usually perpendicular to the length. A regular shaped BTS (100) has a rectangular morphology with the edges parallel either to *b*-axis or *c*-axis, making the third axis (*a*-axis here) 60 degrees out-of-plane. BTS (100) usually has terraces on the surface. BTS (001) has a hexagonal morphology. The edges are usually parallel to *a*-axis or *b*-axis. Terraces and islands easily form on the surface of BTS (001) with hexagonal morphology similar to smaller platelets. A very rough surface is therefore optically visible.

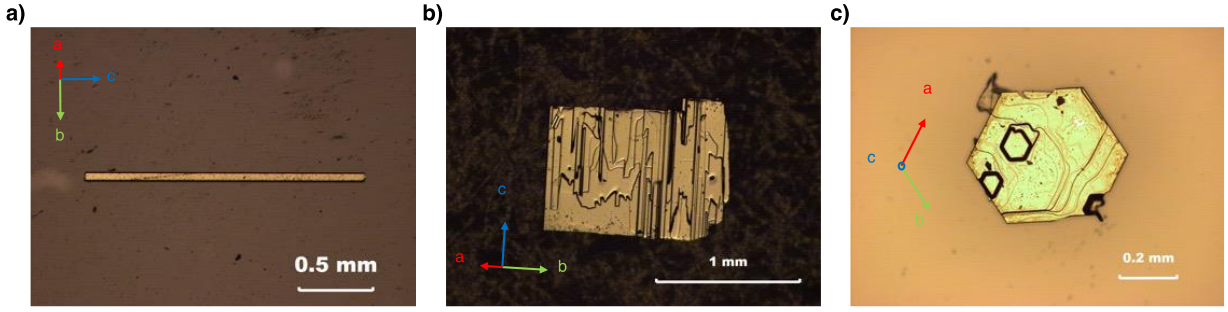

Figure S1. Optical images and crystal orientations of BTS crystals of three morphologies. (a) BTS needle; (b) BTS (100); (c) BTS (001).

II. Out-of-plane and in-plane orientation by thin film XRD

The orientation of the terminating surfaces of BTS are characterized by X-ray diffractometer (XRD) based on the presumed crystalline orientations. Figure S2 c, d, e shows the out-of-plane XRD of BTS needle, BTS (100) and BTS (001), and the insets are the rocking curves for 300 or 002 reflections. The rocking curves are fitted with a gaussian distribution to extract the full width at half maximum (FWHM). XRD of BTS needle and BTS (100) points to the same out-of-plane orientation, thus both structures are terminated by {100} crystalline surfaces. However, the rocking curve of BTS (100) doesn't have a perfect gaussian distribution even if the FWHM of 0.011° is lower than that of BTS needle. This higher mosaicity in BTS (100) plate could originate from small angle domain boundaries inside the crystal, while such domain rarely exists in BTS needles unless it is curved. BTS (001), on the other hand, are easily distinguished from BTS (100) by the difference in the number of 00*l* reflections: Although 00*l* and 0*k*0 reflections are only slightly different in the *d*-spacing (2θ), even numbers of 00*l* reflections of BTS are extinct given the sliding symmetry in $P6_3mc$. The crystal quality of BTS (001) is comparable with other morphologies with a rocking curve of 0.013° FWHM.

The in-plane crystallography orientation of BTS crystals and facets are determined by pole figure studies. Figure S2a, b shows the geometry within a qualitative Ewald's sphere above the sample stage. The crystal is at the center of the hemisphere, while the source and detector are located on the hemisphere and can be moved independently along a longitude circle and thus such plane is the diffraction plane and 2θ is the angle between them. ζ represents the angle between the out-of-plane orientation and the bisector of 2θ. The ϕ is the rotational axis of the goniometer,

perpendicular to the sample stage and the χ is the tilting axis of the goniometer, representing the tilting angle between the rotational axis and the diffraction plane. Out-of-plane orientation will then be defined by $\chi = 0$ in this geometry. Although tilting of 90° can be achieved with χ, samples with platelet geometry lose diffraction intensity dramatically at high tilting angle due to reduced beam projection. Therefore, off-axis reflections close to the out-of-plane are best for in-plane orientation determination.

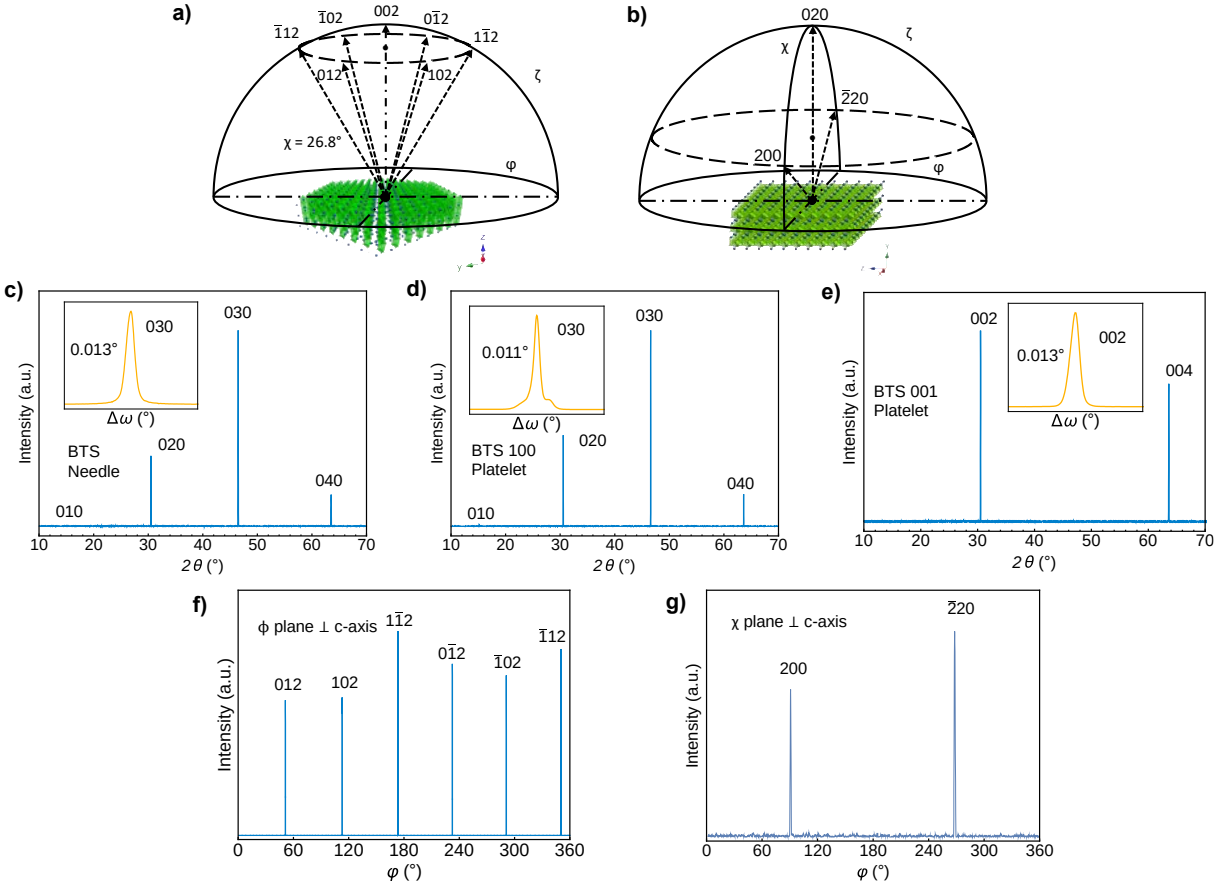

Figure S2. Orientation determination of (100) and (001) BTS plates. (a) XRD geometry for BTS (001). 002 reflects the out-of-plane orientation. 6-fold symmetry is determined by pole figure. Angle between 002 and 012, χ=26.8°, is calculated form the crystal structure; (b) XRD geometry for BTS needle and BTS (100). The out-of-plane orientation is (001). 6-fold symmetry is determined by 60° χ-rotation between 200 and 020 orientations. Thin film out-of-plane XRD and the rocking curve of (c) BTS needle, (d) BTS (001), (e) BTS (100). BTS needle and BTS (100) have the same 0*k*0 orientation and a full width at half maximum (FWHM) of 0.013° and 0.011° in the rocking curve. BTS (100) shows more mosaicity, represented by the asymmetric rocking curve. BTS (001) has a 00*l* orientation, and a rocking curve with FWHM of 0.013°. (f) Pole figure of BTS (001) crystal. 012 off-axis reflections show 6-fold rotational axis perpendicular to ϕ. The asymmetry in the reflection comes from the misalignment; (g) Pole figure of BTS (100) crystal. χ = 60° between 020 and 200 matches the 6-fold symmetry. The in-plane orientation is also determined by a pole figure, while *c*-axis is in the diffraction plane when 200 or $\bar{2}20$ reflection appear.

BTS (001) has 012 off-axis reflections at 26.8° from 002 and shows a six-fold rotational symmetry about 002. To find such reflections, BTS (001) is first aligned towards out-of-plane orientation like we did earlier. Then a tilting angle χ or ζ is set to 26.8° which is carefully examined based on the reference crystal structure. Finally, we set $2\theta = 34.35°$ for 012 reflections (or 2θ angle for 024 if ζ tilting is used) and rotate the crystal with ϕ from 0° to 360°. This will create the pole

figure for BTS (001), and six equivalent reflections given by six-fold symmetry are detected if the crystal is properly aligned (Figure 2f). 100 is therefore lying in the diffraction plane when we are at the center of 012 reflections. Similar method is used for BTS (100) and BTS needle to determine *c*- and *a*-axis. However, one needs to be careful as in-plane reflections ($4\bar{2}2$, $4\bar{2}\bar{2}$, $\bar{4}22$, $\bar{4}2\bar{2}$ and 004, $00\bar{4}$ for example) are almost indistinguishable with 2θ angles lying about 60° away in {100} planes. This will mess up the symmetry determination. We use the primary reflections of *h*00 to tell the in-plane orientations apart. Figure 2g shows the diffraction geometry of the in-plane orientation determination of BTS (100), and the pole figure is shown in Figure 2b. The *c*-axis will be within the diffraction plane when 200 or $\bar{2}20$ reflection appears.

III. Pole figure analysis

To exclude incommensurate superlattices along the primary axes, rotational XRD ζ mapping are done in *a*-*b* and *a*-*c* plane. This is a series of θ-2θ scans with stepped ζ angle. Once the *c*-axis is aligned perfectly parallel to the out-of-plane orientation, a ζ mapping will demonstrate all reflections between 100 and 010 in the *a*-*b* plane (Figure S3a) or *a*-*c* plane if the *a*-axis is parallel to the out-of-plane (Figure S3b). In Figure S3a, 010 orientation is first aligned to the out-of-plane orientation, then rotation b-axis parallel to χ rotational plane. θ-2θ scans from 10° to 60° are carried out for every 1° between χ = -6° to 66°. Peaks are indexed based on 2θ and χ relative to out-of-plane orientation (100 series in this case) and plotted in 2θ space. This verified the six-fold axis to be perpendicular to χ rotational plane. Similar mapping is done for the *ac* plane for χ = -5° to 75°, Figure S3b. No incommensurate structures are seen in the *ab* and *ac* plane. This matches with the reported crystal structure.

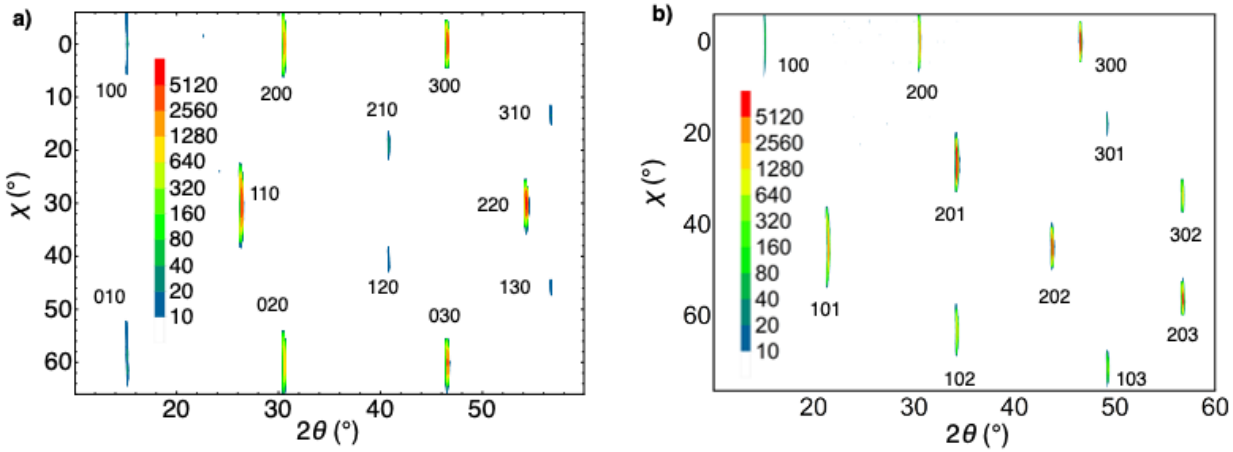

Figure S3. Rotational XRD Mapping (θ-2θ scan and map χ), and sign of superstructure. (a) The *ab* plane. A 60° rotation from 100 to 010 is characterized. Peaks showing up match with diffraction pattern of BTS; (b) The *ac* plane. No incommensurate superstructure shows up along the *a*-axis or the *c*-axis. Structure matches with a stoichiometry $BaTiS_3$.

IV. X-ray absorption spectrometry (XAS) in total electron yield (TEY)

Total electron yield is also monitored in XAS measurements as the compensating current flowing into the sample. Figure S4 a, b show the polarization averaged XAS spectra of BTS (100) and BTS (001) in TEY mode and PFY mode. Because the average electron mean free path at 460 eV is around 1.2 nm[1] while the photon mean free path at 460 eV is estimated as 0.2 μm^2. TEY and PFY XAS is then sensitive to different thickness of BTS crystal: TEY is detecting the first few layers of atoms near the surface while PFY is more sensitive to the bulk down to 0.2 μm. This

comparison indicates the surface states of the as grown BTS crystals are different from the bulk towards higher XAS energy. A reasonable guess is the oxygen absorbance at the surface has stabilizes oxidized states and passivated the surface. We then used PFY mode for BTS XAS analysis to minimize surface states contribution.

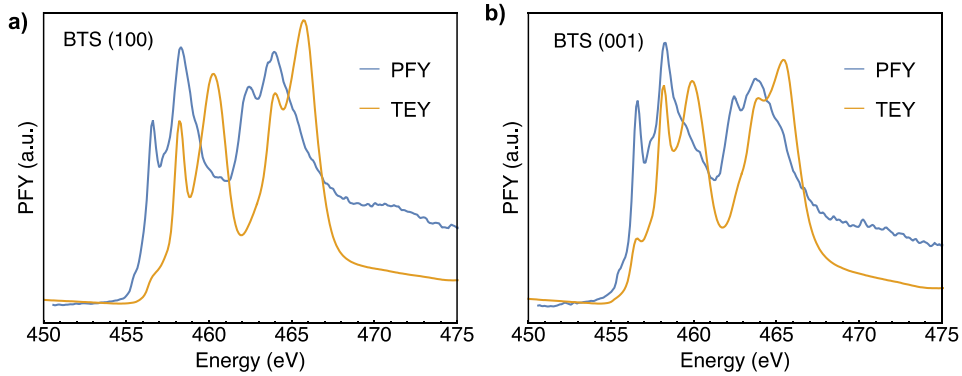

Figure S4. Polarization averaged XAS spectra of (a) BTS (100), and (b) BTS (001) in PFY mode and TEY mode measured simultaneously. TEY shows surface states of higher energy, which is most likely to be oxidized states of Ti near the surface.

V. Additional measurements using Fourier-transform infrared (FTIR) spectroscopy

Unpolarized transmittance spectra of BTS crystals with different morphologies grown at different times were measured in FTIR. BTS crystals were mounted on top of the same sapphire substrate. A blank substrate was then used as the background. Spectra of different crystals were scaled to make a clear comparison in Figure S5. Except for BTS (001), BTS crystals all features two absorption edges at 0.2-0.3 eV and 0.75-0.8 eV. Morphologies and small temperature change within the growth window thus do not change the optical properties of BTS.

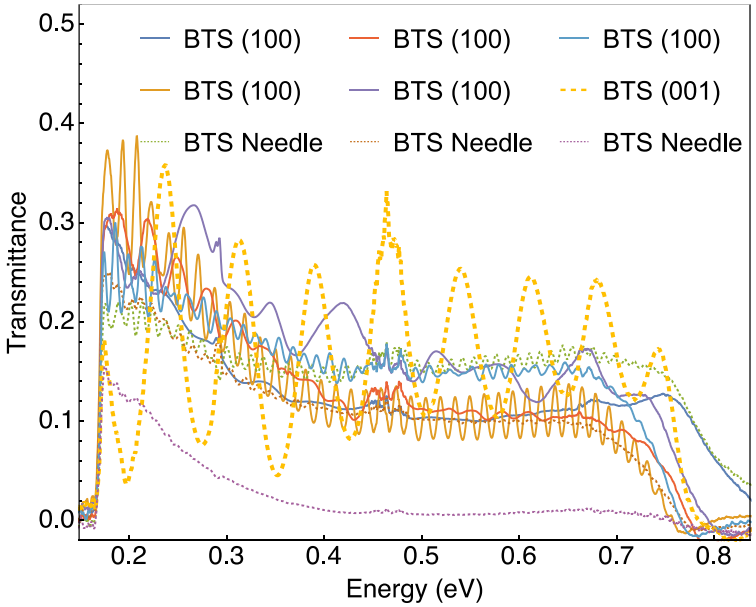

Figure S5. FTIR transmittance spectra of BTS crystals of different morphologies. Two absorption energies exist for BTS needle and BTS (100): 0.76 eV belonging to ordinary ($\perp$ c) and 0.27 eV which is extraordinary ($/\!/$ c). BTS (001) does not show extraordinary transmittance and have only one absorptance edge at 0.76 eV.

(1) Seah, M. P.; Dench, W. A. Quantitative Electron Spectroscopy of Surfaces: A Standard Data Base for Electron Inelastic Mean Free Paths in Solids. *Surf. Interface Anal.* **1979**, *1* (1), 2–11. https://doi.org/10.1002/sia.740010103.
(2) Ravel, B.; Newville, M. *ATHENA* , *ARTEMIS* , *HEPHAESTUS* : Data Analysis for X-Ray Absorption Spectroscopy Using *IFEFFIT*. *J Synchrotron Rad* **2005**, *12* (4), 537–541. https://doi.org/10.1107/S0909049505012719.